Advances towards the Development of a Brain Microwave Imaging Scanner

Syed Ahsan, Maria Koutsoupidou, Eleonora Razzicchia, Ioannis Sotiriou and Panagiotis Kosmas
Department of Informatics, King's College London, London, UK, panagiotis.kosmas@kcl.ac.uk

Abstract—**This paper presents some hardware advances towards a microwave system for brain imaging. In particular, we present a new antenna array design for efficient propagation of microwave signals in the head, as well as a metamaterial structure designed for transmission enhancement through impedance matching. The presented system is modelled in CST Microwave Studio®, using a specific anthropomorphic mannequin (SAM) head model to analyse performance. Simulations results suggest that our designs can be useful in designing a microwave scanner for brain imaging applications such as stroke detection and monitoring.**

Index Terms—**printed monopole antenna, microwave tomography, antenna array CST, brain imaging, metamaterial.**

I. INTRODUCTION

Microwave imaging for medical applications is under extensive research across the globe due to the advantages attributed to electromagnetic (EM) radiation in the microwave spectrum. Microwave tomography methods transmit sequentially and record low-power EM signals propagated into biological tissues, typically in the 0.5-3.0 GHz frequency band. Important milestones towards achieving a functional microwave imaging apparatus include: 1) designing a system with efficient antennas which can operate in the desired frequency range; and, 2) transferring maximum EM energy into the imaging domain [1].

Various antennas designs have been proposed for microwave imaging; for example, radar-based approaches for breast cancer detection have proposed antennas operating in the ultra-wideband (UWB) region from 3.0-12.0 GHz [2]–[5]. In microwave tomography, the profile of the imaging domain is quantitatively reconstructed by processing signals transmitted through the region of interest [6]–[8]. This requires operation in lower frequencies (up to 3.0 GHz), which increases the penetration depth and stability of the reconstruction algorithm. For stroke microwave imaging, theoretical studies have argued that optimal operation is achieved below 2.0 GHz [1], due to the strong attenuation that EM waves experience when propagating inside the head.

To improve signal penetration into the region of interest, a dielectric medium is typically used to couple the energy from the transmitting array. Immersing the antennas into a lossy dielectric has two major advantages: reducing unwanted signals due to antenna coupling and surface and multipath propagation [9], and also broadening the frequency operation range [10]. On the other hand, attenuating the propagated signals to reduce these effects inevitably also impacts the system's ability to detect useful weak signals from the target.

Thus, the use of a matching medium that could couple EM energy into the human body efficiently could have a positive impact on microwave imaging systems. To this end, novel materials such as metamaterials could be used to enhance the energy coupling within the tissue. Candidates for this purpose include split-ring resonators (SRRs), which have been proposed for various microwave applications such as electromagnetic absorbers [11], near-field imaging [12], [13], biosensing [14], [15] and magnetic resonance imaging [16]. SRR-based metamaterials have been used at higher frequencies for improving the impedance matching and absorbing properties of materials [17]. Electromagnetic transmission through a metamaterial that comprises subwavelength rings printed on dielectric substrates depends on the waves polarization and angle of incidence [18].

Based on the above, the aim of this paper is twofold: to present a novel antenna array for microwave brain imaging immersed in a 90% glycerol-water mixture, and to investigate the effect of a SRR-based metamaterial as matching medium for coupling the signals into the head. The metamaterial film is placed on the skin surface to improve microwave transmission towards the brain and to reduce impedance mismatch reflections on the glycerol-skin interface. The remainder of this paper describes our approach in more detail and presents some preliminary results to evaluate its potential for being integrated into a future microwave imaging scanner for the head.

II. ANTENNA DESIGN AND SETUP

The antenna element and array design for our envisioned brain imaging scanner are shown in Fig. 1. The antenna has been modelled in CST Microwave studio. It has been designed on an FR-4 substrate and is based on a triangular patch with a partial ground on the back side. The antenna is fed using an SMA connector connected with a transmission line as shown in Fig. 1. To achieve broadband operation and couple energy more efficiently into the head, the antenna is immersed in a 90% glycerol-water mixture. The dimensions of the patch, substrate, transmission line and partial ground are also shown in Fig. 1. The reflection coefficient S_{11} of the antenna is plotted in Fig. 3(a). The S_{11} values stay below -10 dB for the whole range $0.6 - 2.5$ GHz, with a deep resonance at 1.0 GHz where S_{11} falls below -25 dB.
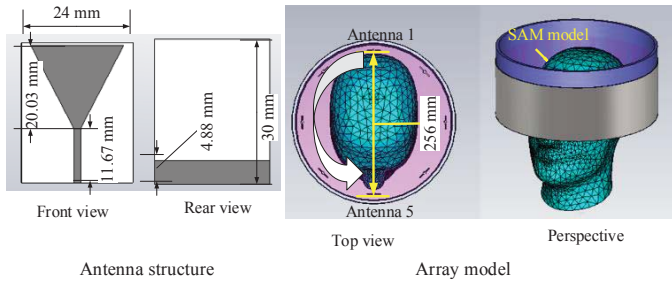
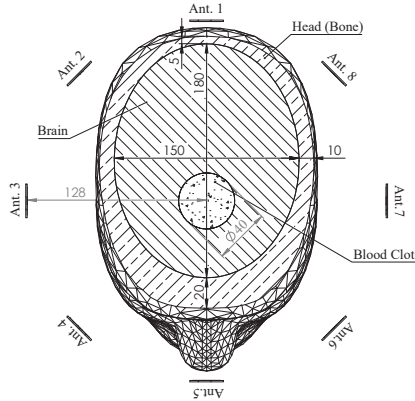Fig. 1: Antenna and array structures modelled in CST Microwave Studio.

Fig. 2: Cross section of the model at the centre plane of the antenna array. The cross section shows blood clot, brain lesion and the remainder of the head comprised of bone material with their respective dimensions in the plane .

We have also modelled an array setup around the head, using CST's EN 50361 Specific Anthropomorphic Mannequin (SAM) Phantom head model. We used this SAM model in our simulations as it can mimic more realistic geometries for microwave measurements. The SAM head model was incrporated using CST's import 3D files Interface. The head region was modelled as a bone shell filled with an elliptical brain shape. The ellipsoid representing brain has a major axis diameter of 180 and minor axis 150 mm (see Fig. 2). We assigned a permittivity value of 45.8 and conductivity of 0.76 S/m to the brain region while for bone these values have been considered as 20 and 0.35 respectively. We also create a large acrylic cylinder covered with an absorber layer comprised of ECCOSORB MCS and a metallic sheet to mimic an imaging tank surrounding the head (see Fig. 1). We filled the acrylic tank with 90% glycerol-water mixture, and subsequently immersed the head model into the tank, as shown in Fig. 1.

III. ARRAY PERFORMANCE

The resulting received signal strengths are plotted in dB as a function of receiver location in Fig. 3(b). The curves are indicative of signal propagation through the model of Figs. 1 and 2 (in the absence of the blood clot). We refer to this

setup, i.e. brain and bone immersed in 90% glycerol, as the 'not target scenario'. Transmitted signal levels are higher than -100 dB for up to 1.0 GHz and higher than -140 dB for up to 2.5 GHz. These parabolic curves are not fully symmetric, with signals at port 5 at higher levels than at the adjacent elements 4 or 6, which suggests complex EM propagation mechanisms for the considered model.
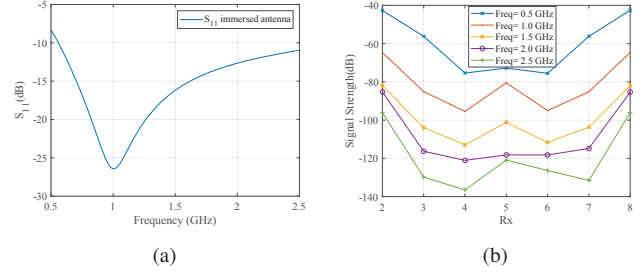

Fig. 3: Reflection parameter (S_{11}) of the proposed antenna, (b) Received signal strength (in dB) as a function of receiver location for Transmitter 1 (as in Fig.1) for 'not target' case.
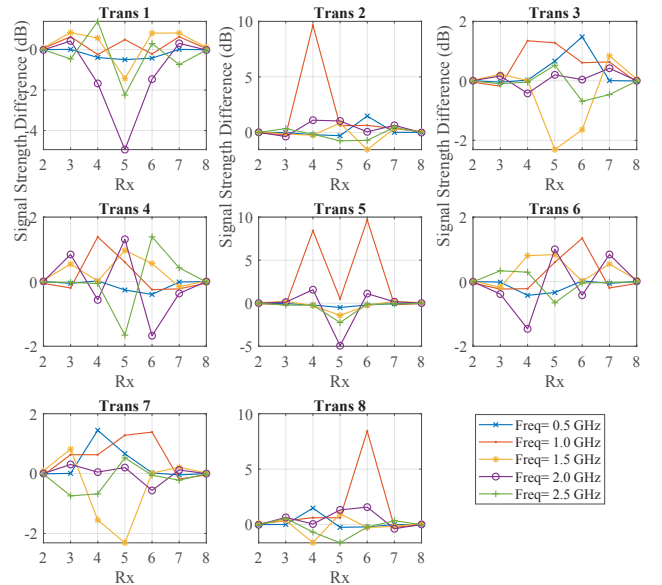

Fig. 4: Received signal strength differences ('target' - 'no target' in dB) as a function of receiver location for each transmitter at discrete frequencies between 0.5 to 2.5 GHz at a step of 0.5 GHz. We subtract the transmitted gains after adding the inclusion from the 'no target' case in dB values.

We have also performed an analysis of signal propagation in the model in the presence of a high contrast dielectric medium mimicking a blood clot inside the brain volume. We considered a cylinder of 4 cm diameter and height to resemble two-dimensional (2-D) scattering scenarios. We assigned dielectric properties of blood from CST's material library to mimic this

discontinuity. As an example, the blood's dielectric constant and conductivity values at 1.0 GHz are 61.0 and 1.56 S/m, respectively. We refer to this scenario (where a high dielectric object is introduced) as 'with target' case. Differences (in dB) in the signal strengths 'with' and 'without' this 'blood clot' are plotted in Fig. 4 for each of the transmitters in the array. As in Fig. 3(b), these differences are plotted as a function of receiver for frequencies from 0.5 to 2.5 GHz with a sample step of 0.5 GHz. The plots in Fig. 4 suggest that differences in signal levels between the 'without target' and 'with target' cases can be as high as 5 dB.

IV. METAMATERIAL MATCHING FILM

A metamaterial film that comprises a lattice of metallic cross-shaped SRRs (SSRs-CS) embedded between two substrates of a high permittivity dielectric ($\epsilon' = 10.2$ and $\tan\delta = 0.0022$), such as Rogers RO3010 ^{TM}, has been designed. Two values were tested for the substrates thickness, according to commercially available options for this laminate: t = 0.64 mm, and the more flexible t = 0.25 mm. The geometrical configurations for a single SRR-CS are shown in Fig.5: the side size of each element is 2.5 mm, the gap length is 0.3 mm, and the distance of the SRRs in the lattice is 0.8 mm.

To simplify this preliminary analysis, the metamaterial was applied to a simpler geometry than the one presented in the previous section, comprising four flat layers: skin (thickness t1 = 6 mm), bone (t2 = 8 mm), cerebrospinal fluid (CSF) (t3 = 1 mm) and average brain (t4 = 20 mm) (see Fig. 5). The dielectric properties of the tissues were found in [19]. A layer of glycerol was added before the metamaterial film (thickness tg = 9 mm, permittivity $\epsilon' = 18$ and conductivity = 1.3 S/m at 1 GHz). The setup was modelled and simulated with CST Microwave Studio® for plane wave excitation of linear polarization and unit cell boundary conditions in the 0.5-1.5 GHz frequency range. The reflection (S11) and transmission (S21) parameters were calculated considering port 1 before glycerol layer and port 2 after brain layer. For evaluating the effect of the SRRs metamaterial the aforementioned setup without the metamaterial was also simulated.

The simulation results are shown in Fig. 6. The use of the thicker film (t = 0.64) improved transmission by 0.7 dB and reflection by 1 dB over the 0.5 to 1.5 GHz frequency range. The thinner and more flexible metamaterial (t = 0.25 mm) leads to a transmission improvement of 0.5 dB over the whole frequency range, while the electromagnetic reflection was reduced in the 0.5-1.0 GHz range and increased in the 1.0-1.5 GHz. The results prove that the use of the metamaterial improves power transmission, although the improvement is still limited. Future work involves optimization of the proposed design and modelling it with more realistic setups, as different polarization and incidence angles will be tested.

V. CONCLUSION

We have presented our recent advances towards the design of a brain microwave imaging scanner. First, we introduced a
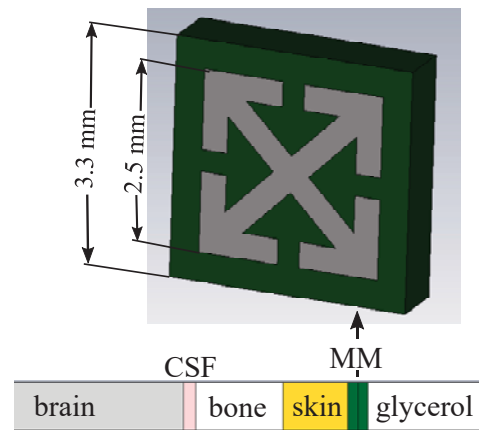

Fig. 5: Geometrical configurations of a single SRR-CS of the metamaterial lattice and the tissue and material layers for the simulation setup.
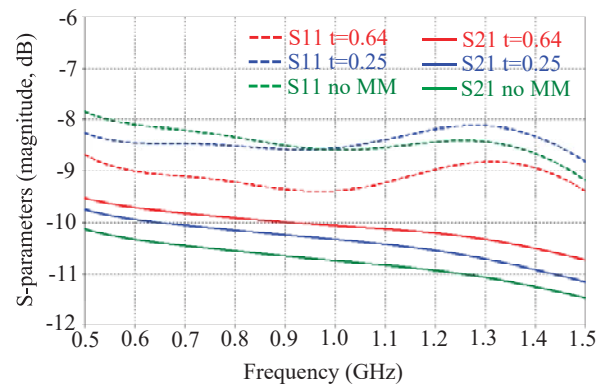

Fig. 6: Simulation results for the transmission (S21) and reflection (S11) parameters for the SRR metamaterial with thick substrates (t = 0.64 mm) (red), the SRR metamaterial with thin substrates (t = 0.25 mm) (blue) and without a metamaterial (green).

new antenna array design and studied its produced signal levels in the presence of a SAM head model in CST. We have shown detectable signal differences (in dB) between the transmitted signals when a high contrast target medium resembling a blood clot was introduced in the head model. This information will be used to test our algorithms for reconstructing the dielectric profile of brain in future work.

Additionally, we also examined the feasibility of developing a SRR based metamaterial film to function as an impedance-matching layer to enhance microwave brain imaging. The SRR-based metamaterial film showed a 0.7 dB improvement in transmission through a simplified layered model. To assess and improve the metamaterial's performance, further designs and simulation studies will be presented in the conference, which will incorporate the metamaterial in the more realistic models for the array and the head.

References

[1] R. Scapaticci, L. Di Donato, I. Catapano, and L. Crocco, "A feasibility study on microwave imaging for brain stroke monitoring," *Progress In Electromagnetics Research*, vol. 40, pp. 305–324, 2012.

[2] E. Porter, M. Coates, and M. Popovic, "An early clinical study of time-domain microwave radar for breast health monitoring," *IEEE Trans.Biomed. Eng.*, vol. 63, pp. 530–539, March 2016.

[3] X. Li, E. J. Bond, B. D. V. Veen, and S. C. Hagness, "An overview of ultra-wideband microwave imaging via space-time beamforming for early-stage breast-cancer detection," *IEEE Antennas Propagat. Mag.*, vol. 47, pp. 19–34, Feb 2005.

[4] E. C. Fear, J. Bourqui, C. Curtis, D. Mew, B. Docktor, and C. Romano, "Microwave breast imaging with a monostatic radar-based system: A study of application to patients," *IEEE Trans. Microw. Theory and Tech.*, vol. 61, pp. 2119–2128, May 2013.

[5] M. Klemm, I. J. Craddock, J. A. Leendertz, A. Preece, and R. Benjamin, "Radar-based breast cancer detection using a hemispherical antenna array -experimental results," *IEEE Trans. Antennas Propag.*, vol. 57, pp. 1692–1704, June 2009.

[6] C. Gilmore, P. Mojabi, A. Zakaria, M. Ostadrahimi, C. Kaye, S. Noghanian, L. Shafai, S. Pistorius, and J. LoVetri, "A wideband microwave tomography system with a novel frequency selection procedure," *IEEE Trans. Biomed. Eng.*, vol. 57, pp. 894–904, April 2010.

[7] P. M. Meaney *et al.*, "Initial clinical experience with microwave breast imaging in women with normal mammography," *Academic Radiology*, vol. 14, no. 2, pp. 207 – 218, 2007.

[8] S. Y. Semenov, R. H. Svenson, A. E. Bulyshev, A. E. Souvorov, A. G. Nazarov, Y. E. Sizov, V. G. Posukh, A. Pavlovsky, P. N. Repin, A. N. Starostin, B. A. Voinov, M. Taran, G. P. Tatsis, and V. Y. Baranov, "Three-dimensional microwave tomography: initial experimental imaging of animals," *IEEE Transac. Biomed. Eng.*, vol. 49, pp. 55–63, Jan 2002.

[9] P. M. Meaney, F. Shubitidze, M. W. Fanning, M. Kmiec, N. R. Epstein, and K. D. Paulsen, "Surface wave multipath signals in near-field microwave imaging," *Int. J. Biomed. Imaging*, vol. 2012, p. 8, 2012.

[10] C. J. Fox, P. M. Meaney, F. Shubitidze, L. Potwin, M. Kmiec, and K. D. Paulsen, "Characterization of an implicitly resistively-loaded monopole antenna in lossy liquid media," *Int. J. Antennas. Propagat.*, vol. 2008, p. 9, 2008.

[11] M. Karaaslan, M. Bağmanci, E. Ünal, O. Akgol, and C. Sabah, "Microwave energy harvesting based on metamaterial absorbers with multi-layered square split rings for wireless communications," *Opt. Commun.*, vol. 392, pp. 31 – 38, 2017.

[12] D. Isakov, C. J. S. , F. Castles, and P. S. Grant, "A split ring resonator dielectric probe for near-field dielectric imaging," *Sci. Rep.*, vol. 7, p. 2038, 2017.

[13] S. Mukherjee, X. Shi, L. Udpa, S. Udpa, Y. Deng, and P. Chahal, "Design of a split-ring resonator sensor for near-field microwave imaging," *IEEE Sens. J.*, vol. 18, pp. 7066–7076, Sept 2018.

[14] A. A. Abduljabar, D. J. Rowe, A. Porch, and D. A. Barrow, "Novel microwave microfluidic sensor using a microstrip split-ring resonator," *IEEE Transac. Microw. Theory Tech.*, vol. 62, pp. 679–688, March 2014.

[15] H.-J. Lee *et al.*, "A planar split-ring resonator-based microwave biosensor for label-free detection of biomolecules," *Sens. Actuators B Chem.*, vol. 169, pp. 26 – 31, 2012.

[16] M. A. Lopez, M. J. Freire, J. M. Algarin, C. Behr, P. M. Jakob, and R. Marqués, "Nonlinear split-ring metamaterial slabs for magnetic resonance imaging," *Appl. Phys. Lett.*, vol. 98, no. 13, p. 133508, 2011.

[17] H.-T. Chen, J. Zhou, J. F. OHara, F. Chen, A. K. Azad, and A. J. Taylor, "Antireflection coating using metamaterials and identification of its mechanism," *Physical review letters*, vol. 105, no. 7, p. 073901, 2010.

[18] P. Markoš and C. M. Soukoulis, "Transmission properties and effective electromagnetic parameters of double negative metamaterials," *Opt. Express*, vol. 11, pp. 649–661, Apr 2003.

[19] D. Andreuccetti, "An internet resource for the calculation of the dielectric properties of body tissues in the frequency range 10 Hz-100 GHz," *Httpniremf Ifac Cnr Ittissprop*, 2012.